

# CHARACTERISTICS OF FLOW INTERACTION AROUND TWO SQUARE PRISMS ARRANGED SIDE-BY-SIDE

I.A. Gad \*, R.M. El-Taher \* and R.M. Atia \*\*

\*Department of Mechanical, Power Engineering, Faculty of Engineering,  
Zagazig University

\*\* The General Jute Product Company, Egypt

## ABSTRACT

The 2-D incompressible flow about two square prisms arranged side-by-side at Reynolds number ( $2 \times 10^4$ ) is simulated by the discrete vortex method (DVM). The shear layers were represented by a number of discrete vortices and the two prisms were represented by the surface singularity method. The flow was assumed to be started impulsively from rest and the flow characteristics were calculated at successive time steps. The time average values of lift, drag, lift amplitude and Strouhal number were calculated at the later stages of motion when the flow became periodic. The calculations have been carried out for several gap ratios. Zones of flow separation, reattachment, wake spread and wakes interference were clarified by visualization of flow around two square models arranged side-by-side in a smoke wind tunnel. For  $G/L < 3.0$ , the results show that the interaction effects increase with decreasing the gap ratio. No serious interaction effects are noticed for  $G/L > 3.0$ .

**Keywords:** Discrete Vortex Method, Flow Interaction, Surface Singularity Method, Sharp Edged Bodies, Square Prism-Flow Visualization.

## INTRODUCTION

When more than one bluff body is placed in a uniform flow, the aerodynamic parameters and vortex-shedding patterns are completely different from the case of a single body, because their wakes or vortex streets interfere in a complex manner, depending on the arrangement and spacing of the bluff bodies. Recent engineering problems have necessitated detailed investigations of aerodynamic characteristics and flow patterns about multiple bluff bodies. Examples of these engineering problems are the local strong wind around a group of skyscrapers, the flow-induced vibration of tubes in heat exchangers, transmission cables, chimney stacks, cooling tower arrays and bridges, marine and offshore structures. The flow induced vibrations may in the end lead to the failure or shutdown of industrial facilities which, in turn, could inflict heavy financial losses or even loss of human lives.

The problems of vortex shedding from bluff bodies have been extensively studied since long time ago. Studies on the problems of wake development and vortex shedding behind a rectangular or square prism in free-stream flows have recently been investigated both numerically and experimentally by Kelkar *et al.* [1], Sarpkaya *et al.* [2] and Davis *et al.* [3].

Experimental investigations on the fluid flow and heat transfer around rectangular prism were carried out by Igarashi [4]. The 2-D Navier-Stokes and continuity equations for time dependent incompressible viscous flow about single square prism was treated experimentally and numerically in an infinite domain by Davis *et al.* [3]. The numerical method utilized third order upwind differencing for convection and a Lieth type of temporal differencing. Wind tunnel tests for a single square were carried



out. The Reynolds number regime investigated is from 100 to 2800.

Previous investigations of the flow interference problem about multiple bluff bodies have been carried out experimentally, especially on flows around groups of circular cylinders as in References 5 to 8. Very little numerical investigations, using DVM, for treating the flow interference about bluff bodies for high Reynolds number exist [9, 10]. In parallel to the present work. El Gohary [11] applied a general finite difference algorithm using a hybrid scheme for the convective terms to solve the unsteady, two dimensional incompressible Navier-Stokes equations for viscous flow past two circular cylinders arranged side-by-side and in tandem. The stability of this exact solution was limited by  $Re$  of  $O[10^3]$ .

The present work concentrates on the modeling of separated low speed flows around two square prisms arranged side-by-side at  $Re=2 \times 10^4$  using the DVM. The aim is to gain more understanding of the fundamental physics of this type of flow and to make further refinements for the DVM in studying flow interference about bluff bodies.

**MATHEMATICAL MODEL**

The interference flow between two square prisms arranged side by side with gap ratios  $G / L$  in a uniform stream (Figure 1) is treated. The flow is impulsively-started at time  $t=0$ . The Reynolds number is sufficiently large so that the flow can be simulated by an inviscid model. The eight separated shear layers from the corners of the two bodies are approximated by DVM. Each shear layer is represented by an array of discrete point vortices which are shed near the corner at appropriate time intervals and introduced and convected by the flow field into the wake. The surface singularity method is used to represent the two bodies,[12]. Each body is replaced by number of bounded vortices and the shear layers replaced by free discrete vortices as shown in Figure 2.

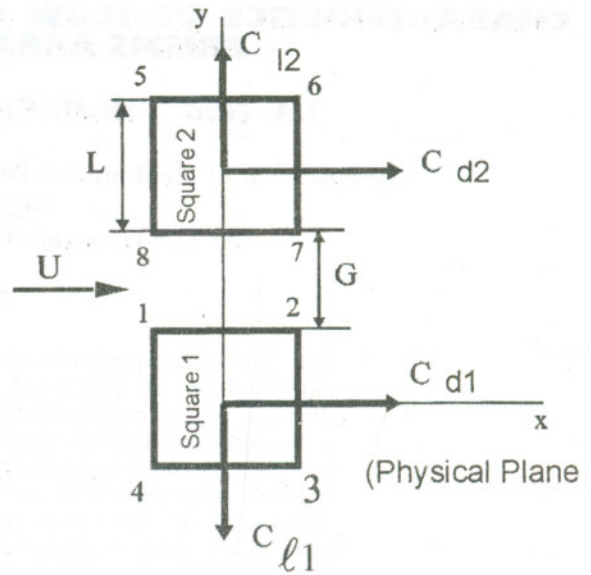


Figure 1 Flow About Two Square prisms arranged side-by-side with gap ratio  $G/L$

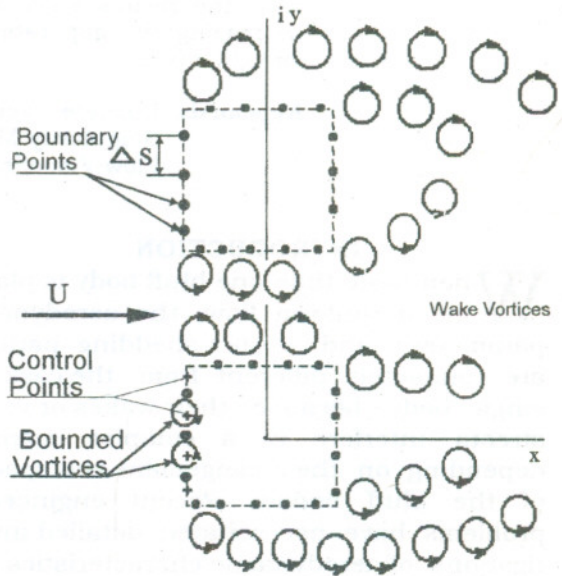


Figure 2 Flow field representation.

The complex potential is the superposition of the uniform stream, bounded vortices square 1 and square 2, and wake vortices (eight shear layers) emanated from the eight corners of



the two squares The flow field complex potential function can be written as follows:

$$F(Z) = -UZe^{-i\alpha} + \sum_{\lambda=1}^2 \sum_{j=1}^N \frac{i\Gamma_{c\lambda j}}{2\pi} \text{Ln}(Z - Z_{c\lambda j}) + \sum_{\eta=1}^8 \sum_{\beta=1}^{M_\eta} \frac{(-1)^\phi i\Gamma_{\eta\beta}}{2\pi} \text{Ln}(Z - Z_{\eta\beta}) \quad (1)$$

Equation 1 can be normalized by dividing both sides by UL and both values of L and U are taken equal unity. So the time and the strengths of Vortices are nondimensionalized. The nondimensional complex velocity at any nonsingular point is given by :

$$-u + iv = \frac{dF(Z)}{dZ} = -Ue^{-i\alpha} + \sum_{\lambda=1}^2 \sum_{j=1}^N \frac{i\Gamma_{c\lambda j}}{2\pi(Z - Z_{c\lambda j})} + \sum_{\eta=1}^8 \sum_{\beta=1}^{M_\eta} \frac{(-1)^\phi i\Gamma_{\eta\beta}}{2\pi(Z - Z_{\eta\beta})}$$

$\phi=1$  for clockwise vortex rotation,  $\phi=2$  for anticlockwise vortex rotation.

A surface vorticity distribution must make the velocity on the inside of the body vortex sheet zero and the contour a streamline [12 and 13]. As a consequence the normal velocity on the contour is also zero. The velocity on the outside of the sheet is equal to the vortex sheet strength. Satisfying the zero-internal tangential velocity condition at the midpoint of each segment (called control point) generates a set of N simultaneous linear equations for each of the two bodies:

$$[k_{\lambda ij}] [\gamma_{c\lambda j}] = [-b_{\lambda j}] \quad (3)$$

$K_{\lambda ij}$  is the coupling coefficient of the influence matrix  $[K_{\lambda ij}]$  for one body,

$-b_{\lambda j} = U'_j$  is the onset tangential velocity at the  $j^{\text{th}}$  control point.

The singularity of  $[K_{\lambda ij}]$  is removed by replacing one equations of the system by Kelvin condition for inviscid flow. This condition must be satisfied for each body

separately [14]. Kelvin theorem for each body is:

$$\sum_{j=1}^N \gamma_{c\lambda j} \Delta s_{\lambda j} = -\Gamma_{\lambda e} \quad (4)$$

The Gaussian elimination method is used here for each system (Equation 3 represents two systems,  $\lambda=1,2$ ). A suitable iteration scheme is used for treating the coupling between the two simultaneous systems. At the start of each time step eight nascent vortices are introduced at a distance  $d_\eta$  away from its separation corner. The strength of  $\eta^{\text{th}}$  nascent vortex is:

$$\Gamma_{o\eta} = 0.5 V_{sh\eta}^2 \Delta t \quad (5)$$

where,  $V_{sh\eta}$  is shear-layer velocity at the  $\eta^{\text{th}}$  separation edge, taken equal the tangential velocity at the control point nearest to the  $\eta^{\text{th}}$  corner of the face along which the flow separates. The sign of the nascent vortex is determined by the relative magnitudes of the velocities at the two faces adjacent to the corner [15]. The position  $d_\eta$  satisfying Kutta conditions (velocity = 0.0 at the sharp edged point) is [2]:

$$d_\eta = \frac{1}{2\pi} V_{sh\eta}^2 \Delta t \quad (6)$$

The second order-convection scheme is used for the convection of the free vortices as follows:

$$Z_{\eta\beta}(t + \delta t) = Z_{\eta\beta}(t) + 0.5((u_{\eta\beta} + iv_{\eta\beta})_t - (u_{\eta\beta} + iv_{\eta\beta})_{t-\delta t}) \delta t \quad (7)$$

All the calculations for convection are repeated every  $\delta t = \Delta t / 2$ .

Two mechanisms simulating some viscous effects are used in this paper. The vortices which approach too close to any solid boundary will ordinarily be dissipated by the action of viscosity. These vortices are removed from the calculations whenever they come closer than its core radius from body surface. The chaotic motion of vortices (the vortices of opposite circulation could remove themselves from the wake at high speeds when they are in close proximity)



was avoided by coalescing such vortices for  $M > 20$  when their cores touch i.e. by combining the two vortices into an equivalent single vortex.

Generalized Blasius theorem [16] is used to calculate the forces exerted on each square as:

$$X_{d\lambda} + iY_{d\lambda} = \frac{1}{2} i \rho \oint_{\lambda} (dF/dZ)^2 dZ + i \rho \frac{\partial}{\partial t_{\lambda}} \oint F dZ \quad (8)$$

The time variant force coefficients are defined as:

$$C_{d\lambda} = X_{d\lambda} / \frac{1}{2} \rho U^2 L, C_{l\lambda} = Y_{d\lambda} / \frac{1}{2} \rho U^2 L.$$

To have a convenient comparison between the forces acting on the two squares,  $C_{l1}$  was taken equal to  $-Y_1 / \frac{1}{2} \rho U^2 L$ . The time average force coefficients calculation:  $\bar{C}_1, \bar{C}_d$  and  $S_t$ , for each square have been carried out at the later stage of the motion ( $M > 30$ ) where the transient behavior disappears. The Strouhal number is calculated from  $C_1$  curve as the inverse of the average time period [2].

#### UNCERTAINTY ANALYSIS

The selection of an optimum time interval is of primary importance in achieving relatively time-step insensitive results and in saving computation time. In the present analysis the optimum time step  $\Delta t$  (nondimensional) is determined by repeating some trial calculations for the case of a single square with only the time step changed. Experiments on  $\Delta t$  began with  $\Delta t = 0.02$  and were repeated with  $\Delta t = 0.04, 0.06, 0.08, 0.12, 0.16, 0.20,$  and  $0.24$ . The results showed that  $\Delta t = 0.24$  is too large and that the results with  $\Delta t = 0.04, 0.06, 0.08, 0.12,$  and  $0.16$  did not significantly differ. However, the computation time required with  $\Delta t = 0.04$  was more than six times larger than that with  $\Delta t = 0.06$ .

Two convection schemes (first and second order) for convection of the free

vortices were tested, separately, for different values of  $\Delta t$ :

$$x(t + \Delta t) = x(t - \Delta t) + 2\Delta t u(t)$$

$$x(t + \Delta t) = x(t) + 0.5[3u(t) - u(t - \Delta t)]\Delta t$$

For small  $\Delta t = 0.12, 0.08, 0.07, 0.04$  and  $0.02$  the results did not lead to any noticeable differences. As shown in Reference 2, the first scheme has an error in any time step of order  $\Delta t^2$  and the second has an error of order  $\Delta t^3$ . In order to save computer time; it was decided to take  $\Delta t = 0.16$ . ( $\Delta t$  taken by the previous investigators was in the same range [2]). The last scheme is used in the present investigation to minimize the error in convection process. A new vortex is introduced into the wake every  $\Delta t = 2\delta t$  and all the calculations for convection are repeated every  $\delta t$ .

In the same manner, numerical experiments on the number of boundary vortices  $N$  began with  $N = 20$  and were repeated with  $N = 40, 80, 160$  and  $240$ . The results showed that taking  $N = 80$  or higher did not affect the results. The estimation of the shear layer velocity at the separation edge from the tangential velocity near to but not at the edge (at which the velocity is either 0 or  $\infty$ ) seems to be likely inaccurate and strongly depend on  $N$  (or on  $\Delta s$ ).

Coalescence and removal techniques are an approximation and there is no "correct" or "guaranteed" way to perform it. One should use it with care and, if possible, verify that it did not introduce unacceptably large errors. In the present work, numerical experiments for separation distances used for coalescence and removal ( $h_1$  and  $h_2$  respectively) were repeated by changing  $h_1$  and  $h_2$  separately. The results showed two optimal intervals for each distance:  $h_1/L = [0.025:0.038]$  and  $h_2/L = [0.034:0.05]$ . For all values of  $h_1$  and  $h_2$  out side these intervals, the results are not smooth and suffer from high jitters. Previous results [14], showed that the core radius of a decaying line vortex which has been in the wake of a viscous flow with  $Re = 4 \times 10^4$  is of the order of  $0.025L$ .



**VISUALIZATION OF FLOW**

The two square prism models used for flow visualization test are made from wood. Each model is 100 mm height and 13 mm length of the square cross-section. The two models are painted black. The tunnel is made of steel sheets, and is mounted vertically on a light tubular steel trolley. The air flow is induced by means of a fan driven by variable speed electric motor at the top of the tunnel. Air enters the base of the tunnel by way of a muslin strainer and is led

through a contraction cone to the working section. The working section is 180 mm wide, 240 mm height, and 100 mm deep as seen in Figure 3, and the flow is vertically upwards. Models are attached to the rear wall of the working section while the front wall is of perspex and is readily movable. Smoke is introduced by a comb located below the working section that emits twenty-three streams of smoke at 7 mm center distances.

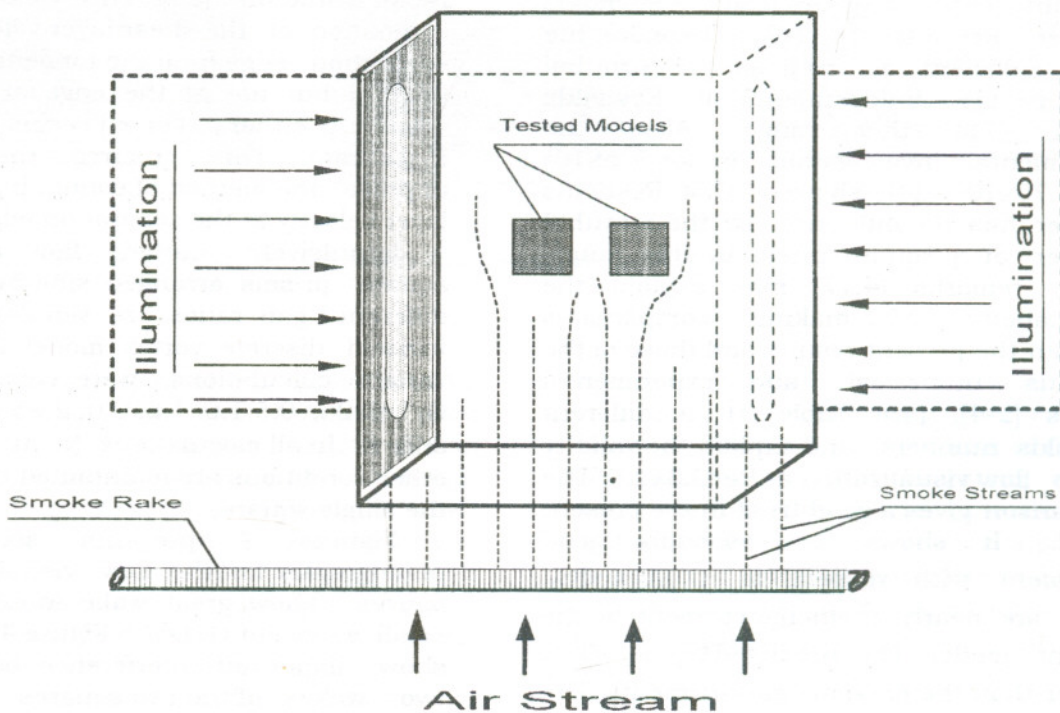


Figure 3 Principal Sketch of smoke tunnel test section

The comb may be traversed from side to side to assist in the detailed exploration of the filed of flow. The working section is brightly illuminated from both sides and the flow pattern could be clearly visible. The air flow velocity in the working section may be varied from zero to about 3 m/s.

In order to obtain a clear picture with more accurate details the following technique is applied in the present work. A video camera is used to view and record the

smoke- visualized flow pattern around the two models arranged side by side for different gap ratios. The video tape is inserted into video system, which is connected to personal computer system through video card. The output video picture is seen on the computer's monitor, and then is captured using oak capture utility program. This system's unique advantage of variable slow-motion-playback, still framing, and slow-motion reverse playback allowed a



detailed and clear picture of the flow pattern. The captured flow pattern pictures are printed using laser jet printer.

### RESULTS AND DISCUSSION

The trial calculations applied to the single square prism showed that a number of bounded vortices,  $N=160$  and time interval,  $\Delta t=0.16$  are appropriate to DVM analysis. Achenbach [17] showed that at subcritical flow condition, in the case of flow around circular cylinder, the wake width as well as dimensionless base pressure remain constant, over a large range of the Reynolds number,  $Re=3 \times 10^4: 4 \times 10^6$ . Therefore the drag coefficient as well as the Strouhal number are independent of Reynolds number in this range. Also, the experimental investigations in for  $7.5 \times 10^3 < Re < 3.75 \times 10^4$ , [4] showed that Reynolds number has no influence on the Strouhal number of a square prism in this range. These remarks [4,17] may explain the reasonability of making comparisons between the present results and those of the previous numerical and experimental results [2-4], (see Table 1) at different Reynolds numbers, and explain the validity of the flow visualization at  $Re=2.3 \times 10^3$ . The comparison gives a good trust in the present model. It shows a reasonably good agreement with respect to  $\bar{C}_1, \bar{A}_1$  and  $S_t$  which are nearly predicted correctly by the present model. The predicted  $\bar{C}_d$  is 15 % greater than the previous measurements. The removed vorticity at the walls of the square is nearly 62% of the vorticity loss while 38% is lost by the combination process. The deviation of the results may be explained as follow: The used coalescence process to

regularize the solution is an approximation and there is no "guaranteed" way to perform it. One should use it with care and, if possible, verify that it did not introduce unacceptably large errors. Unfortunately, it is often difficult to assess the more elusive effects of merging on the numerical predictions since the problem is highly nonlinear and since its consequences are intermingled with those of many other parameters and ad hoc assumptions. On the other hand it is known that the tangential velocity near the separation edge has very rapid variation [15]. This yields that the estimation of the shear layer velocity at the separation edge from the tangential velocity near to but not at the edge (at which the velocity is either 0.0 or  $\infty$ ) seems to be likely inaccurate. This ensures the need to improve the method of estimating the shear layer velocity at the separation edge.

Impulsively started flow about two square prisms arranged side-by-side with different gap ratios are simulated by the inviscid discrete vortex model DVM. Time variant calculations were carried out for  $G/L=0.25, 0.5, 1.0, 1.5, 2.0, 2.25, 3.0, 4.0, 6.0$  and 8. In all calculations  $N, \Delta t, Re$  and all other conditions are maintained the same as the single square.

Figures 4 presents six selected photographs for the flow visualization. The figures show great wake interference for small gaps. For  $G/L=2.5$  Figure 4-e does not show important interference between the two wakes of the two squares. This agrees with the DVM results and adds more trust in the validity of the DVM in treating this type of flow interaction.



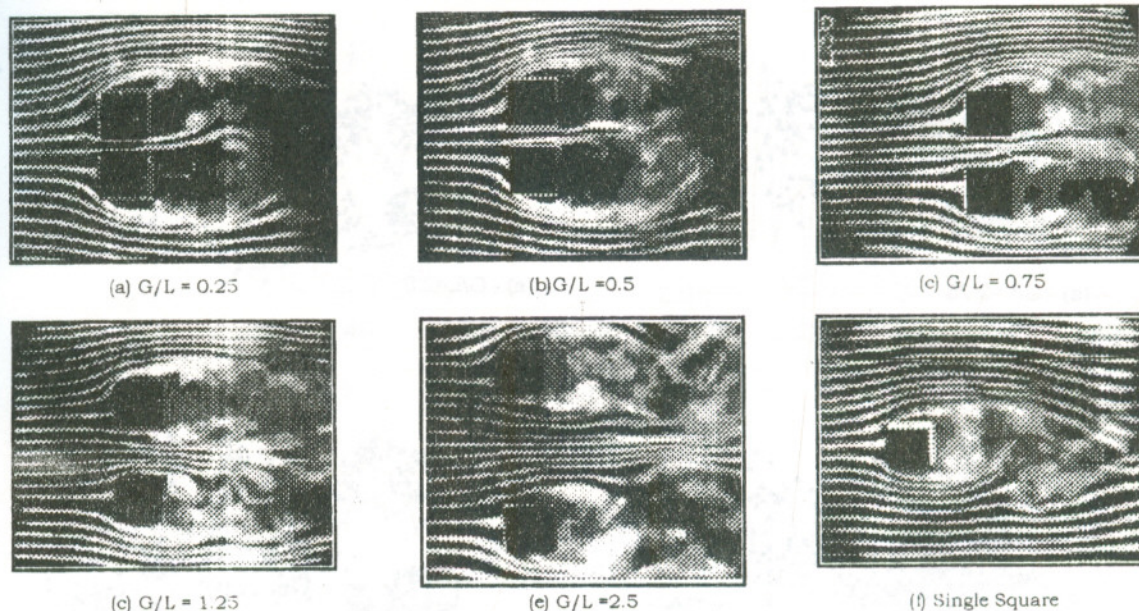


**Figure 4** Visualization of Flow around Two Square Prisms arranged Side by Side for Different Gap Ratios- $Re = 2.3 \times 10^3$ .

The wake configurations (calculated by DVM) behind the two squares were represented at the instant  $t=85$  for all gap ratios in Figure 5, and Figures 5-a through 5-f indicate great wake interference for small gaps. This interference becomes not noticeable for  $G/L > 3$ . For small gaps, both the DVM and the Visualization results showed that the gap flow is biased towards one square, (Figure 4-a, Figure 5-a and Figure 5-b). Biased gap flow is associated with two unequal size near wakes. The flopping phenomenon (switching of the biased gap flow, alternately between the two prisms) is noticed during the calculation and the visualization, but it is not completely studied. The time variant lift coefficient for the lower square was presented for all gap ratios in Figure 6.

Figure 6-a through Figure 6-h show that the periodicity of the lifting force coefficient disappears for narrow gaps due to the steep development of the interaction effect. A comparison between the time variant lift coefficient for the two squares is presented in Figure 7 for four gap ratios (0.25, 0.5, 1.0 and 3.0). Figure 7-d indicates a pronounced phase shift between the two curves with negligible difference in amplitude and mean value. Some variation in the mean value are noticed in Figures 7-a and 7-b. This is due to the biased gap flow and its flopping phenomenon. The time variant drag coefficient for the lower square at all gap ratios is presented in Figure 8. The comparison between time variant drag coefficient for the two squares is presented in Figure 9.



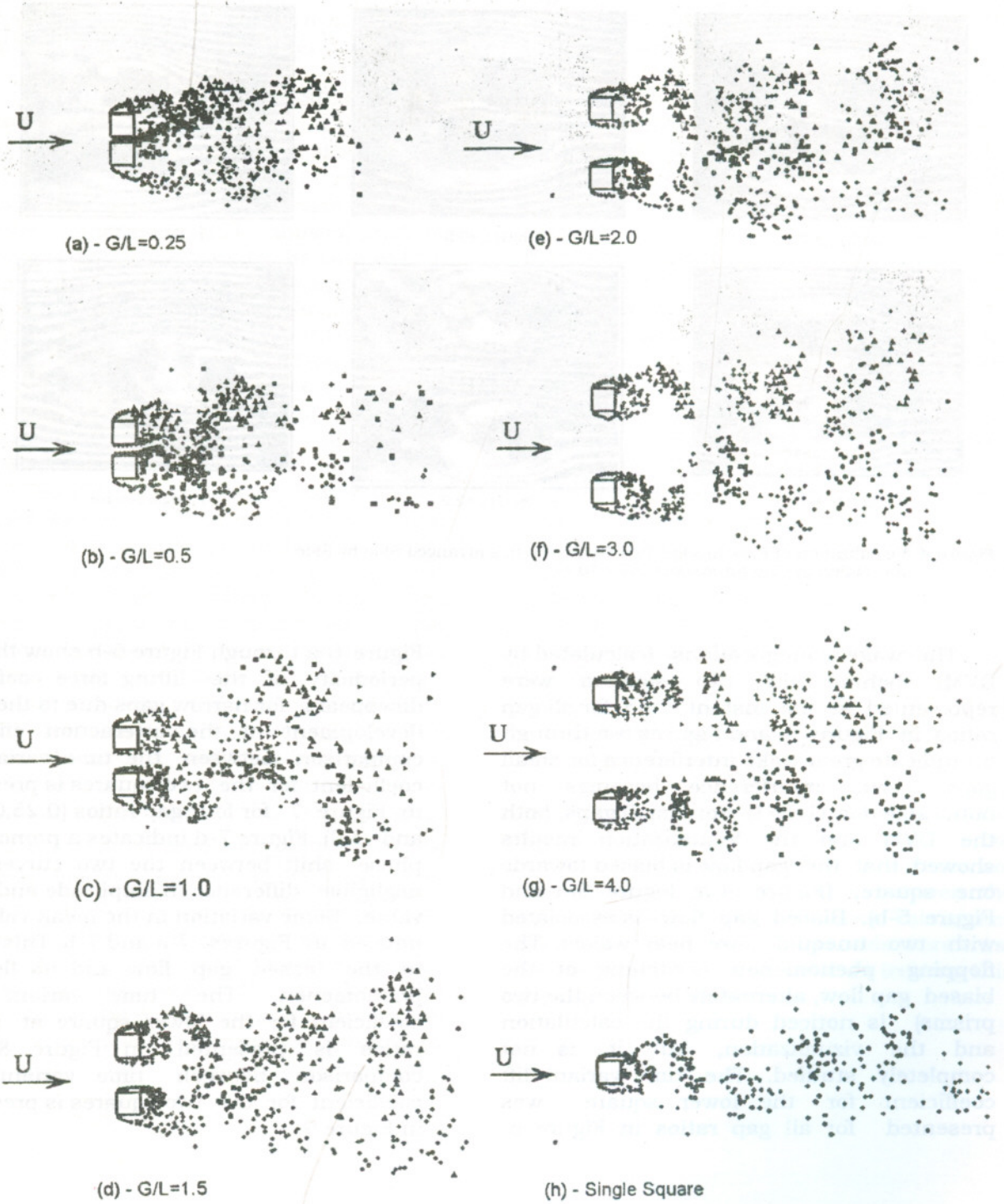


Figure 5 Wake configurations behind the two squares at the instant  $t=85$  for different gap ratios



Characteristics of Flow Interaction Around Two Square Prisms Arranged Side-By-Side

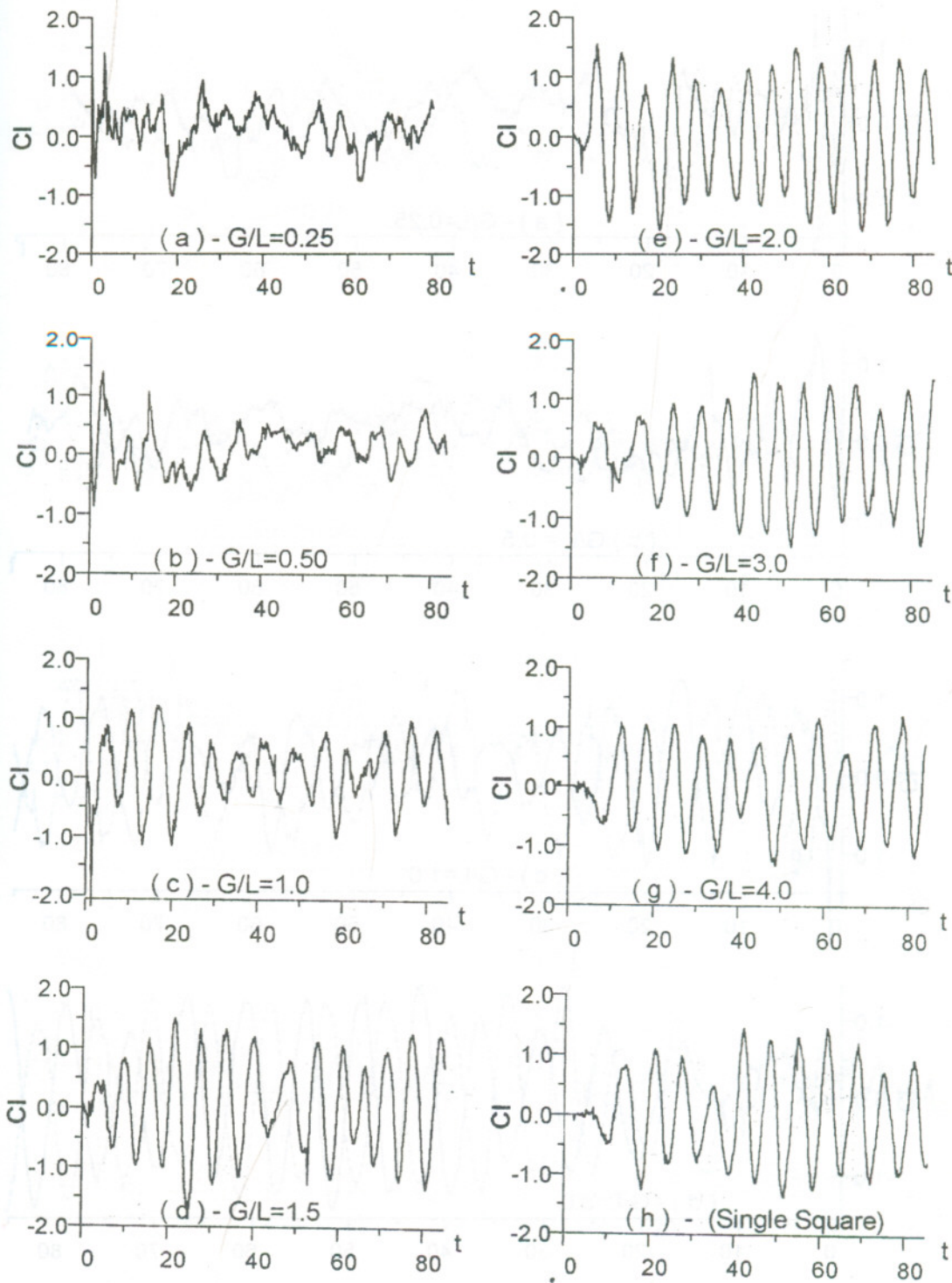


Figure 6 Time variant lift coefficient for square 1 at different gap ratios.



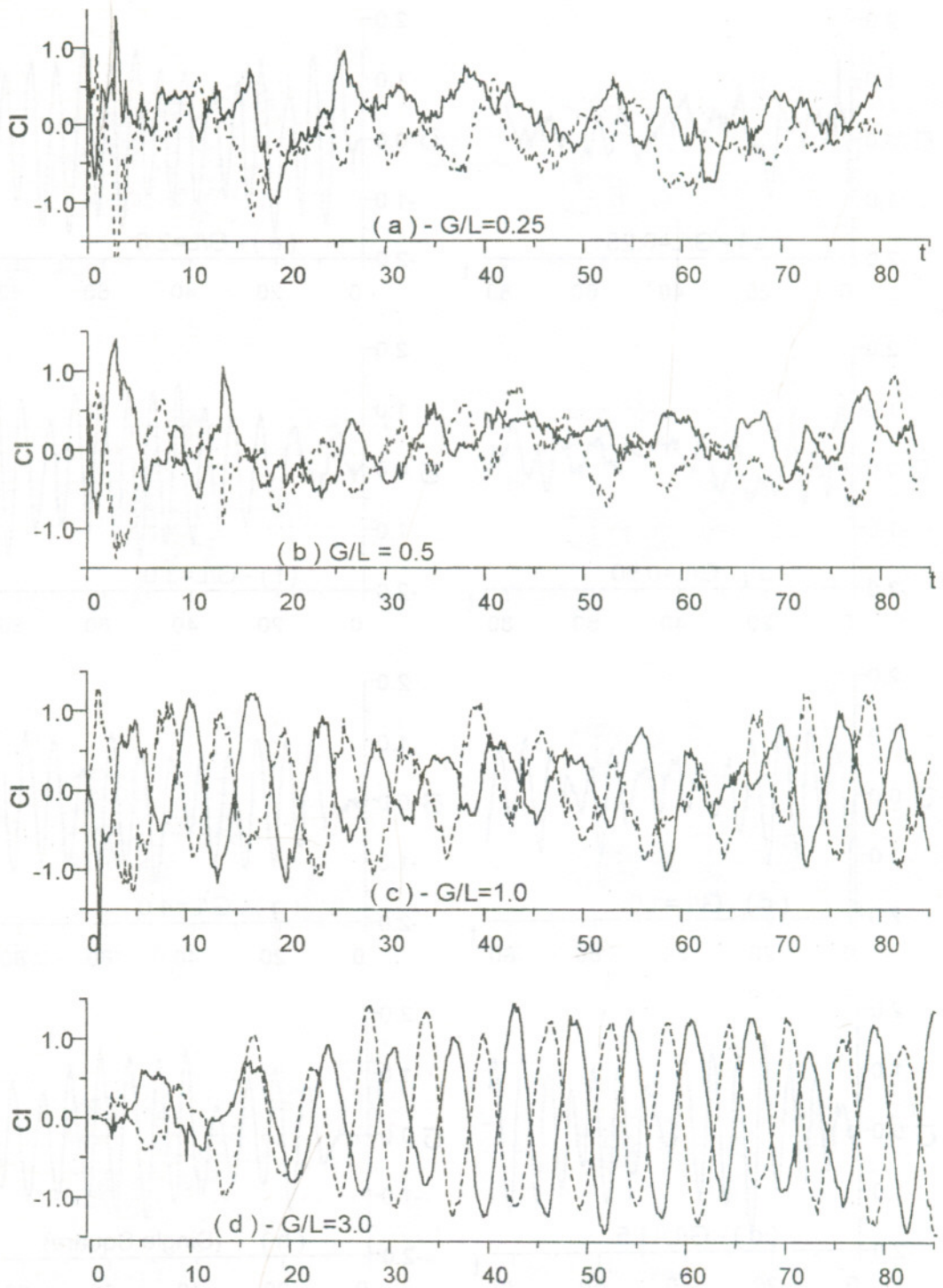
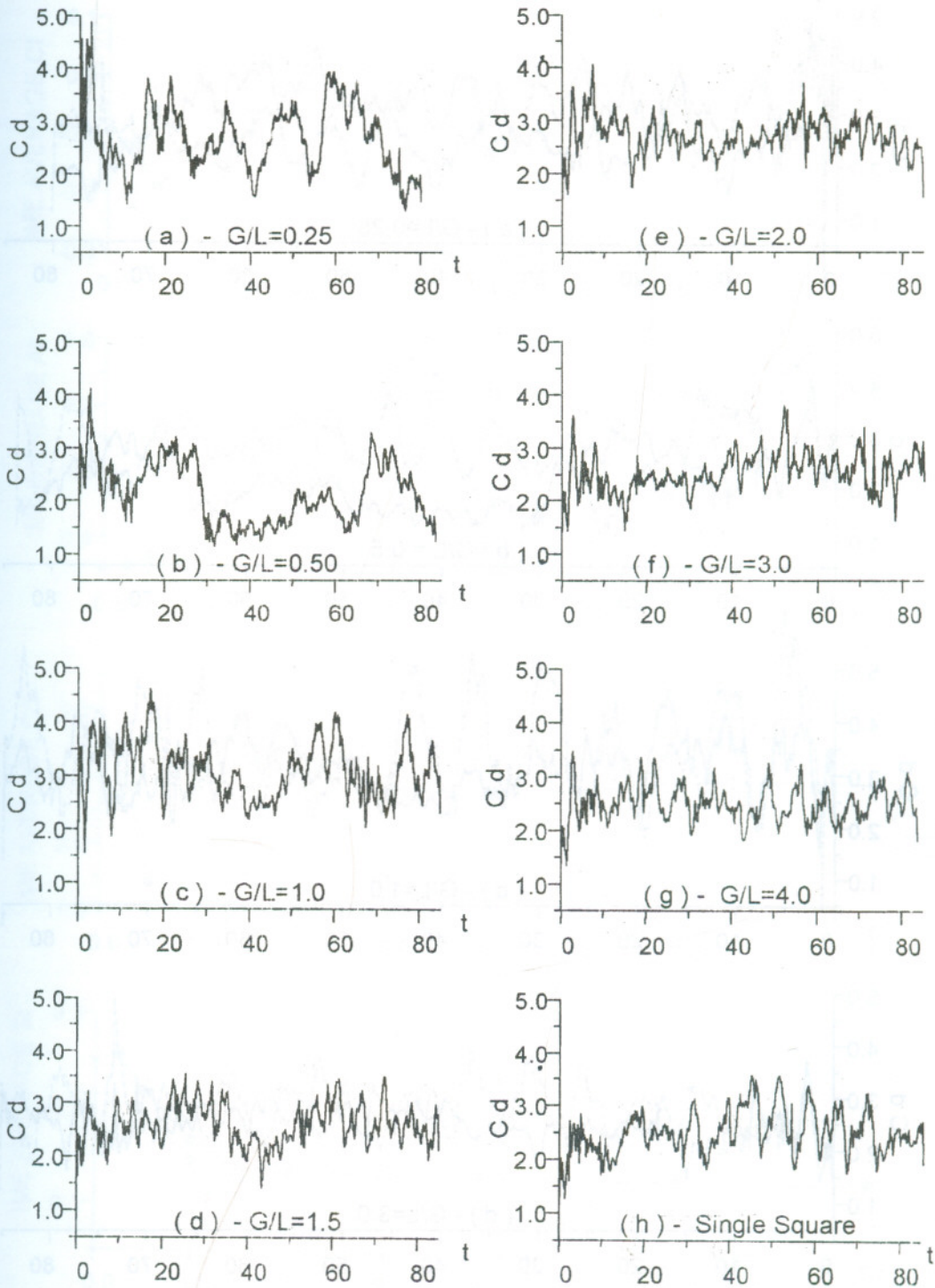


Figure 7 Comparison between time variant lift coefficient for the two squares at different gap ratios; ( \_\_\_\_\_ square 1  
 - - - - - square 2)



# Characteristics of Flow Interaction Around Two Square Prisms Arranged Side-By-Side



**Figure 8** Time variant drag coefficient for square 1 at different gap ratios.



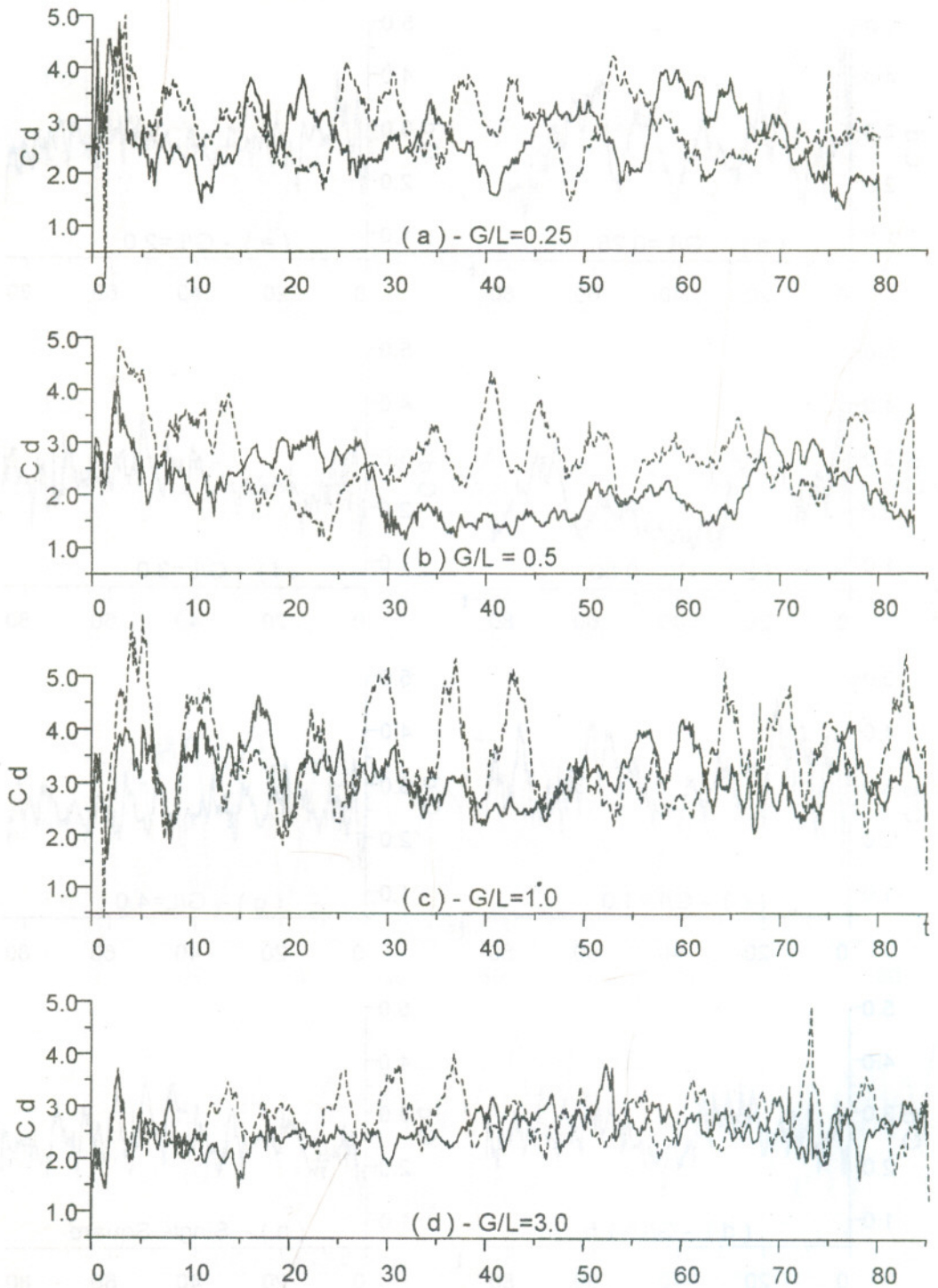


Figure 9 Comparison between time variant drag coefficient for the two squarest gap ratios. (—— Square 1, - - - -Square 2)

Characteristics of Flow Interaction Around Two Square Prisms Arranged Side-By-Side

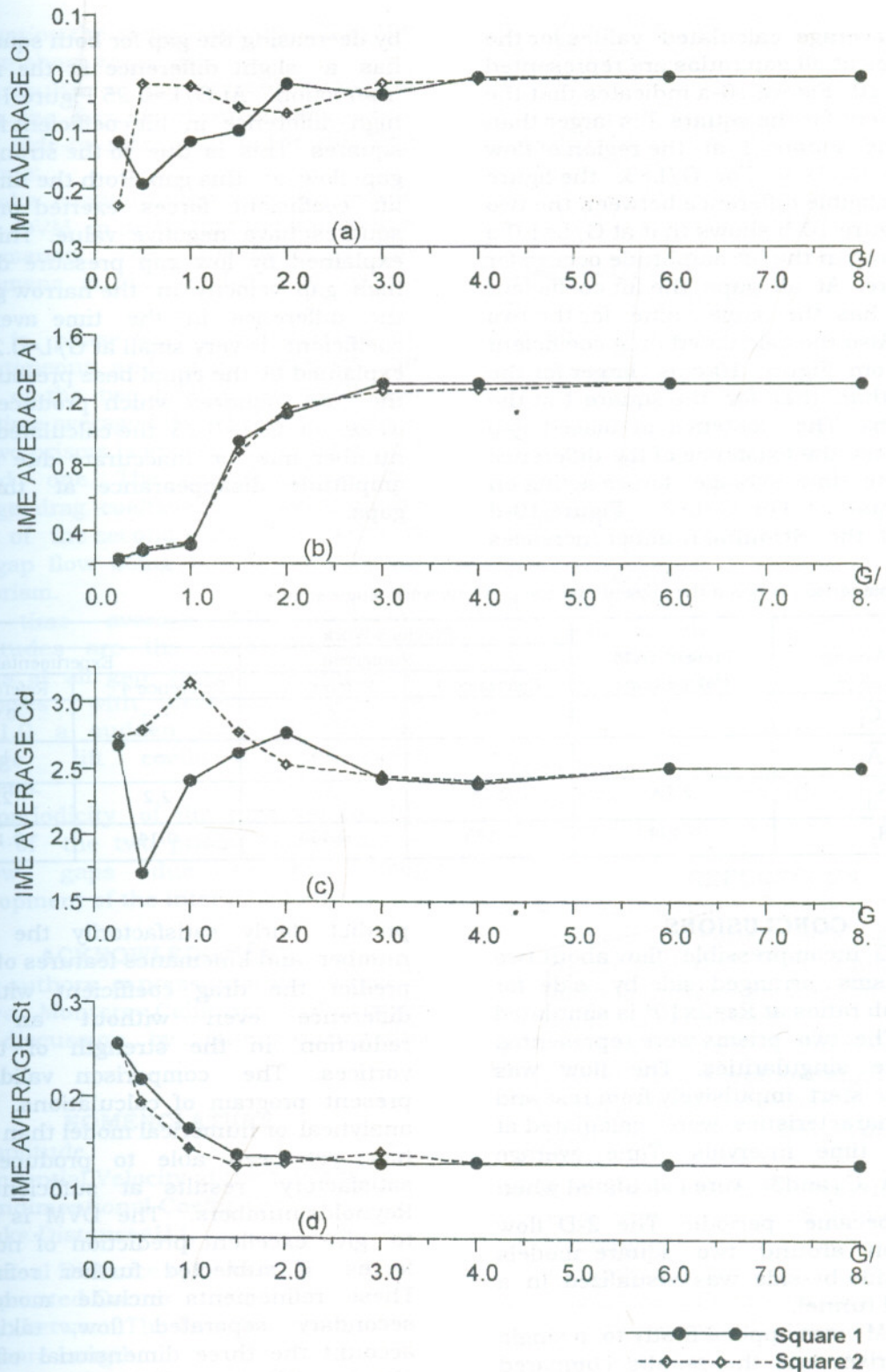


Figure 10 Time average values for the two squares versus gap ratio.



The time average calculated values for the two squares at all gap ratios are represented in Figure 10. Figure 10-a indicates that the lift coefficient for the square 2 is larger than that for the square 1 at the region of flow interaction ( $G/L < 3$ ). For  $G/L > 3$ , the figure shows negligible difference between the two curves. Figure 10-b shows that at  $G/L = 1.0$  a sudden drop in the lift amplitude occurs for both square. At all gaps the lift coefficient amplitude has the same value for the two squares. Also the calculated drag coefficient as seen from Figure 10-c is larger for the square 2 than that for the square 1 at the narrow gaps. The existence of biased gap flow explains the existence of the difference between the time average forces acting on the two squares. For  $G/L < 3$  Figure 10-d shows that the Strouhal number increases

by decreasing the gap for both squares but it has a slight difference at the regions of interaction. At  $G/L = 0.25$  Figure 10-a shows high difference in lift coefficient for the two squares. This is due to the strongly biased gap flow at this gap. Both the time average lift coefficient forces exerted on the two squares have negative value. This may be explained by low gap pressure due to the high gap velocity in the narrow gap. While the difference in the time average drag coefficient is very small at  $G/L = 0.25$  may be explained by the equal base pressure behind the two squares which produce a single wake. At  $G/L = 0.25$  the calculated Strouhal number may be inaccurate due to the lift amplitude disappearance at this narrow gaps.

**Table 1** Comparison between the present and the previous work-single square.

Time Average Values	Present DVM Calculations	Previous Work			
		Numerical		Experimental	
		Reference 4	Reference 3	Reference 4	Reference 2
$\bar{C}_l$	0.01	----	----	----	0.02
$\bar{A}_l$	1.32	----	----	----	1.2
$\bar{C}_d$	2.53	2.18	----	2.2	2.2
$S_t$	0.128	0.146	0.133	0.14	0.125

### CONCLUSIONS

The 2-D incompressible flow about two square prisms arranged side-by-side for different gap ratios at  $Re = 2 \times 10^4$  is simulated by DVM. The two prisms were represented by surface singularities. The flow was assumed to start impulsively from rest and the flow characteristics were calculated at successive time intervals. Time average values  $\bar{C}_l, \bar{A}_l, \bar{C}_d$  and  $S_t$  were calculated when the flow became periodic. The 2-D flow configuration around two square models arranged side-by-side was visualized in a smoke wind tunnel.

The DVM was applied firstly to a single square prism and the results compared with the previous numerical and experimental work. The present calculations

predict fairly satisfactorily the Strouhal number and kinematics features of flow and predict the drag coefficient within 15% difference even without an artificial reduction in the strength of the shed vortices. The comparison validates the present program of calculations. No other analytical or numerical model than the DVM has yet been able to produce equally satisfactory results at sufficiently large Reynolds numbers. The DVM is expected to give excellent prediction of normalized forces if subjected further refinements. These refinements include modeling the secondary separated flow, taking into account the three dimensional effects and viscous diffusion and improving the method



for estimating the shear layer velocity at the separation sharp edge.

The results of the present numerical study for the flow about two square prisms arranged side-by-side lead to the following conclusions:

- The wake configurations show the power of the DVM in predicting the biased flow phenomenon. The instability of this phenomena is also predicted at certain gaps.
- There is phase shift and difference in instantaneous and mean values of lift (drag) of the two prisms. At small gaps, the time average lift coefficient for one of the two prisms is greater than that of the second one. The corresponding time average drag coefficient is lower than the value of the second prism. This is due to the gap flow being biased towards the first prism.
- The time average lift coefficient amplitudes are the same for the two prisms at all gap ratios. This amplitude decreases with decreasing gap. At  $G/L=1.0$  a sudden drop in the time average lift coefficient amplitudes happens.
- The periodicity of the time variant lift force of the two prisms disappears at narrow gaps due to the steep development of the interaction effects.

#### ACKNOWLEDGMENT

The authors express thanks to Prof. T. Sarpkaya., Monterey, California, U.S.A. for his useful discussion by letters during this study.

#### NOMENCLATURE

- A : Amplitude  
 B : Tangential Velocity at the Surface  
 C : Nondimensional Coefficient  
 D : Wake Distance= $U \cdot t_f$   
 D : Normal Distance of  $\Gamma_0$  from Separated Corner  
 G : Gab between The Two Squares  
 L : Square Length  
 M : Number of free Vortices in a Shear Layer  
 N : Number of Bounded Vortices

- Re : Reynolds Number  
 St : Strouhal Number  
 T : Normalized Time  
 U : Free Stream Velocity  
 u,v : Velocity Components  
 X,Y : Force Components  
 x,y : Axes Coordinates  
 Z : Complex Variable = $x+iy$

#### Greek Letters

- $\alpha$  : Incidence Angle  
 $\Delta s$  : Segment Length  
 $\Gamma$  : Vortex Strength  
 $\gamma$  : Vortex Sheet Strength  
 $\eta$  : Number of Shear Layer  
 $\lambda$  : Number of Square Prism

#### Subscripts

- b : Boundary Points  
 c : Control Points  
 d : Drag Force  
 e : total circulation shaded from Body  
 l : Lifting Force  
 o : Nascent Vortices  
 r : Real

#### Over Bars

- Over a variable : average value  
 In equations : complex conjugate

#### REFERENCES

1. K.M. Kelkar and S. Patankar, "Numerical Prediction of Vortex Shedding behind a Square Cylinder", International Journal for Numerical Methods in Fluids, Vol.14, pp.327-3341, (1992)
2. T. Sarpkaya and C. J. Ihrig, "Impulsively Started Flow about Rectangular Prisms: Experimental and Discrete Vortex Analysis", J. Fluids Eng., Vol. 108, 47-54, (1986)
3. R. W. Davis and E. F. Moore "A Numerical Study of Vortex Shedding from Rectangles" J. Fluid Mech. Vol. 116. pp. 475-506, (1982)
4. T. Igarashi, "Fluid Flow and Heat Transfer around Rectangular Prisms (The Case of a Width/Height ratio of a section of 0.33: 1.5)", Int. J. Heat Mass Transfer Vol. 30. No. 5, pp. 893-901, (1987)



5. P.W. Bearman and A.J. Wadcock, "The Interaction between a Pair of Circular Cylinders Normal to a Stream", *J. Fluid Mech*, Vol. 61, pp. 499-511, (1973)
6. R. M. El-TaHER, "Experimental Study of the Interaction between a Pair of Circular Cylinders Normal to a Uniform Shear Flow", *J. Wind Eng. and Ind. Aero.*, Vol. 17, pp. 117-132, (1984)
7. A. Okajima and K. Sugitani "Fluid Characteristics of a Pair of Circular Cylinders Normal to a Uniform Flow at Very High Reynolds Numbers", *Bull. Res. Inst. Appl. Mech.*, Kyushu University, Vol. 53, pp. 37-64, (1980)
8. M. M. Zdravkovich, "Review of Flow Interaction between Two Circular Cylinders in Various Arrangements", *Trans. ASME, I. J. Fluid Eng.*, Vol. 99, pp. 618-632, (1977)
9. G. Bosch and W. Rodi, "Simulation of Vortex Shedding past a Square Cylinder near a Wall", *Proceedings 10th Symposium on Turbulent Shear Flows*, Pennsylvania State University, pp.4.13-4.18, (1995)
10. R.H. Robert and Y. Chia-Chi, "A Numerical Study of Vortex Shedding from a Square Cylinder with Ground Effect", *ASME Journal of Fluid Engineering*, Vol.119, pp.512-518, (1997)
11. H.M. El Gohary, "Numerical Study on Viscous Flow Past Two Circular Cylinders", Ph.D. Thesis, Zagazig University, (1997)
12. B. Hunt, "The Mathematical Basis and Numerical Principles of The Boundary Integral for Incompressible and Potential Flow Over 3-D Aerodynamic Configurations", In: *Numerical Methods in Applied Fluid Dynamics* (B.Hunt, ed.) Academic press, 47-135, (1980).
13. P.K. Stansby and A.G. Dixon, "Simulation of Flow around Cylinders by a Lagrangian Vortex Scheme", *App. Ocean Res*, Vol. 5, pp. 167-178, (1983)
14. T. Sarpkaya, "Vortex Element Method for Flow Simulation", *Advances in Applied Mechanics*, Vol. 31, pp.113-247, (1994)
15. J.M.R. Graham, "Application of The DVM to The Computation of Separated Flows" In: *Numerical Methods for Fluid Dynamics II*, Clardon Press, Oxford 7, pp.273-302, (1986)
16. L.M. Milne-Thomson, "Theoretical Hydrodynamics" 5<sup>th</sup> Ed, The Macmillan Co, New York, (1968)
17. E. Achenbach, "Total and Local Heat Transfer from a Smooth Circular / in Cross-Flow at High Reynolds Number", *Int.J. Heat Mass Transfer*, Vol. 18, pp. 1387-1396, (1975)

Received July 14, 1998  
Accepted May 8, 1999

## دراسة تداخل السريان حول منشورين مربعي المقطع ومتلاصقين

ابراهيم على مصطفى جاد \*، رفعت محمد الطاهر \*، رائد ابراهيم عطية \*\*

\* كلية الهندسة - جامعة الزقازيق

\*\* الشركة العامة لصناعة الجوت - مصر

### ملخص البحث

استخدمت طريقة الدوامات المتقطعة لدراسة تداخل السريان اللامنضغط ثنائي البعد حول منشورين مربعي المقطع عموديين على اتجاه سريان الهواء بجانب بعضهما البعض، حيث يتم تمثيل الطبقات الجدارية المنفصلة عن المنشورين عند الأركان الثمانية إلى دوامات حرة متقطعة تسبح مع السريان، ويتم تمثيل الجسمين بعدد من الدوامات المقيدة على السطح، بنيت الحسابات على أساس أن السريان بدأ صدمياً، وتم حساب خصائص السريان في فترات زمنية قصيرة متتالية، بعد الوصول إلى حالة السريان الترددي المنتظم تم حساب الخصائص المتوسطة للسريان، تكررت الحسابات لمسافات مختلفة بين الجسمين.

باستخدام نفث هوائي دخاني تم عمل رؤية للسريان حول نموذجين للجسمين بغرض مقارنة النتائج العملية بالحسابية. المقارنة مع الأعمال السابقة أكدت الثقة ببرنامج الحساب الذي تم إنشاؤه في هذه الدراسة، كما أكدت قدرة طريقة الدوامات المتقطعة في دراسة تداخل السريان بين الأجسام والظواهر المصاحبة له.